Visible luminescence improvement of ZnO/PAA nano-hybrids by silica coating

Y. Zhang, T. Gard, C. Theron, A. Apostoluk, K. Masenelli-Varlot, B. Canut, S. Daniele, B. Masenelli

Visible luminescence improvement of ZnO/PAA nano-hybrids by silica coating

Y. Zhang[1], T. Gard[2], C. Theron[3], A. Apostoluk[1], K. Masenelli-Varlot[4], B. Canut[1], S. Daniele[2], B. Masenelli[11*]*

[1]Institut des Nanotechnologies de Lyon (INL-UMR5270), Université de Lyon, INSA-Lyon, ECL, UCBL, CPE, CNRS, 69621 Villeurbanne, France

[2]C2P2-CPE Lyon, Université de Lyon, CNRS-UMR 5265, 69616 Villeurbanne cedex, France

[3]Lotus Synthesis SAS, 110 rue Faÿs, 69100 Villeurbanne, France

[4] Université de Lyon, INSA-Lyon, UCBL, MATEIS, UMR CNRS 5510, 69621 Villeurbanne, France

Abstract

The effect of a silica coating on the improvement of the visible light emission properties of ZnO/polyacrylic acid (PAA) nanohybrids is reported. The synthesized material consists of ZnO nanocrystals incorporated into the PAA mesospheres and then coated with silica. The silica amount can be controlled by the concentration of ammonia used in the sol-gel process as catalyst. The interaction between PAA and ammonia is crucial, the presence of the former tending to inhibit the catalytic action of the latter. We show that there is an optimum in the silica amount around the mesospheres, which leads to a drastic increase in the defect-related visible photoluminescence quantum yield of ZnO nanocrystals. A six-fold increase of the quantum yield can thus be achieved, reaching competitive values higher than 60%. This optimum is a compromise between a complete protective silica layer around the mesospheres and too thick a layer inducing inefficient absorption of excitation light by the coating.

Keywords: ZnO nanohybrid, PAA, visible luminescence, silica coating

Introduction

Crystalline defects are often luminescence quenching centers in semiconductors. However, some are also good emitters, such as NV centers in diamond or vacancies in SiC. These atomic defects can be so efficient that they can act as single photon sources [1, 2, 3, 4]. This is the case in ZnO, which is known to exhibit a rich luminescence in the visible range due to the contribution of several types of defects. Several studies have shown that this luminescence can indeed be very intense with a high quantum yield

Corresponding authors :* bruno.masenelli@insa-lyon.fr; *stephane.daniele@univ-lyon1.fr

[5,6,7,8,9,10]. Defect-based visible luminescence can therefore be foreseen as a potential alternative source of visible light. With a wide bandgap of 3.34 eV, ZnO can be promising for down-shifting of the UV light to visible one. ZnO is often characterized by deep defects such as oxygen vacancy (V_O) and shallow defects such as zinc interstitial (Zn_i), which have been assigned as the main sources of the broad-band emission in the visible range [11,12,13,14,15]. The defect configuration is significantly modified when the size of the ZnO samples is reduced to the nanometer scale. In particular, defects at the surface of ZnO nanocrystals become the dominant factor in determining the optical properties of ZnO. Surface states, including defects and adsorbed groups (e.g., OH groups), are strongly dependent on synthesis (in case of chemical methods) [16,17]. Therefore, many researches on ZnO nanostructures have focused on the control and study of surface states. A core-shell structure offers multiple functions to nanoscale materials in terms of catalytic, optical and magnetic properties. The shell can change the charge, functionality and reactivity of the surface, or improve the stability and dispersibility of the core material [18]. Silica is one of the most common shell candidates due to its relative ease of preparation, good environmental stability and compatibility with other materials (allowing biocompatibility [19]). Silica coating on ZnO is a feasible strategy for improving the optical properties of ZnO nanostructure.

The introduction of the silica coating on ZnO nanoparticles is however, rather difficult, due to the large difference in surface energy and the large surface area of ZnO nanoparticles [20]. Two strategies based on Stöber method can be used for the introduction of the silica coating: one during the growth process of ZnO, the other one after growth [21,22]. In the first method, the growth of ZnO takes place simultaneously with the gelation of silica to form a composite. In the second route, previously prepared ZnO nanoparticles are added to the silica gel. Other techniques such as spray drying, magnetron sputtering, spin coating have also been utilized for silica coating [23,24,25]. Regardless of the synthesis process, the presence of silica can affect the shape, size and dispersion of ZnO nanoparticles, and eventually their optical properties.

We have previously developed a hybrid organic/inorganic material made of ZnO nanocrystals embedded in self-assembled polyacrylic acid (PAAH) 3D mesospheres (~ 50 to 100 nm). [26] This material appears to be an efficient visible light emitter. In particular, we have shown that our self-assembled organic/inorganic system can enhance the visible luminescence of ZnO nanocrystals, resulting in a photoluminescence quantum efficiency (PL QY) of 20 % in routine [26]. However, PL QY still needs to be improved and made robust over long a period of time. Moreover, one of the promising applications of such a material is its use as a rare earth-free phosphor for white light-emitting diodes (WLEDs), which also requires high performance for operating temperatures of up to 100-120 °C. For both challenges, in analogy with what has been observed for ZnO nanocrystals, an additional silica coating over the mesospheres embedding ZnO nanocrystals could prove to be beneficial too. In the present study, we aim at investigating the effects of a silica coating on the optical properties of ZnO/PAA nanohybrids as a function of the amount of silica. The latter is controlled essentially by the concentration of ammonia

introduced during the coating synthesis as a catalyst. A new question arises concerning the influence of this catalyst on the self-assembled mesospheres. Indeed, the presence of numerous -COOH functions induces an additional difficulty, as they react with ammonia. Two previous articles from Fuji *et al.* [27] and Wan and Yu [28] showed the elaboration of hollow silica nanospheres from tetraethyl orthosilicate (TEOS) in the presence of PAAH.

Experimental methods

$ZnEt_2$ solution (15%wt in toluene), PAAH (MW = 2000 $g.mol^{-1}$, 63 wt% in water), tetraethyl orthosilicate (TEOS), NH_4OH aqueous solution (32% wt) and anhydrous ethanol were purchased from Sigma-Aldrich and used as received. Deionized water was obtained from ion exchange resin (Lenntech, 1-10 MΩ.cm). ZnO/PAA hybrid mesospheres of about 50-100 nm embedding wurtzite ZnO nanocrystals with a size of about 10 to 20 nm were synthesized as described in our previous works [26, 29]. Typically, the synthesis was performed at room temperature by reacting 1.8 mL of $ZnEt_2$ and 25 mL of 0.63 wt% of polyacrylic acid (PAAH) aqueous solution. The obtained materials are composed roughly of 50 % PAAH and 50 % ZnO from TGA analysis.

Silica coating synthesis

ZnO/PAA samples were then coated by sol-gel process using TEOS and water as reactants and OH^- as catalyst. In a typical coating process, 1.15 g (5.52 mmol) of TEOS was added to the suspension of 300 mg of ZnO/PAA powder (1.84 mmol of ZnO) in 1g of ethanol with constant stirring at 700 rpm at room temperature. The resulting molar ratio TEOS:ZnO being equal to 3, the sample will be denoted TEOS-3. After 30 min of stirring, 2 ml of a mixed solution of EtOH:H_2O:NH_4OH of mass ratio 1:0.93:0.027 were added to the suspension. The stirring continued at 700 rpm at room temperature for additional 4 hours to obtain the final suspension. The resulting white solid was recovered by centrifugation and then washed twice with ethanol and dried for 4 hours at 70 °C. The same experiments without ZnO/PAA and only PAAH or with different amount of NH_4OH were also carried out. Samples with molar ratio TEOS:ZnO fixed at 3 but with different amounts of NH_4OH will be referred to as TEOS-3-1, TEOS-3-2, *etc.*, where the second numbers represent the multipliers of 0.027 NH_4OH nominal mass ratio in the mixed solution of EtOH, H_2O and NH_4OH, while the amounts of EtOH and H_2O are fixed.

For each sample of coated nanohybrids, the corresponding sample of identical uncoated nanohybrids was kept and used as a reference for characterizations. Since both samples contained identical nanohybrids, we can accurately probe the effect of the presence of silica alone in the coated sample, independent of any variation resulting from the initial mesosphere batches, by comparing both samples (reference and coated).

Characterizations

Structural and optical properties were examined for samples of both silica-coated and uncoated ZnO/PAA nanostructures. For structural characterization, X-ray diffraction (XRD) was performed on a Bruker AXS D8 diffractometer using Cu K_α radiation in the Bragg-Brentano configuration; transmission electron microscopy (TEM), high-resolution TEM (HRTEM), high angle annular dark-field (HAADF) imaging and energy dispersive X-ray spectroscopy (EDS) were performed on JEOL 2010F microscope operating at 200 kV. The samples were dry-deposited onto a holey carbon TEM grid. The experimental conditions (magnification, electron dose, dwell time in HAADF and EDS) were chosen in order to minimize irradiation damage in PAA and subsequent oriented attachment of ZnO nanocrystals. The crystal structure, size and morphology were revealed by XRD and TEM. The chemical composition of selected samples was analyzed by Fourier transform infrared spectroscopy (FTIR, Bruker Vertex 80) and Rutherford backscattering spectroscopy (RBS) using a 2 MeV $^4He^+$ ion probe. For optical characterization, photoluminescence (PL) and PL quantum yield (PL QY) were measured at room temperature for each powder sample, which was manually pressed onto an indium foil. The excitation source was a continuous laser at 266 nm (8 mW, Crylas FQCW 266-10) and the emission was detected using a liquid N_2-cooled Si CCD camera after dispersion in a spectrometer (iHR Triax 320 Jobin-Yvon, grating blazed at 500 nm, 600 grooves/mm, spectral accuracy ± 1 nm). PL QY measurements were performed using an integrating sphere, with an internal coating made of spectralon, according to the protocol developed by de Mello *et al*. [30] PL excitation (PLE) was performed on a fluorescence spectrometer (FLSP920, Edinburgh Instruments) from 200 nm to 400 nm (with a spectral width of ± 1 nm) at emission wavelength of 550 nm ± 1 nm. The optical properties were also tested at higher temperatures (up to 100 °C) and the excitation wavelength was chosen at 340 nm ± 2 nm from a Xenon lamp. The emission was detected by a CCD camera (ANDOR NEWTON 970) after dispersion in a monochromator (Triax 320 Jobin-Yvon, 300 grooves/mm, precision ± 2 nm). The intensity variation was monitored by integrating the entire emitted spectrum. All the collected spectra were corrected by the corresponding instrumental function.

Results and discussion

Structural analyses

In the typical conditions and a molar ratio TEOS:ZnO of 3, gravimetric studies conducted without ZnO/PAAH, with the corresponding amount of PAAH (150 mg) and with ZnO/PAAH (300 mg) are summarized in table 1.

Table 1: SiO_2 yield (%) depending on the synthesis conditions

NH_4OH mass (g)	**0.027**	**0.054**	**0.081**	**0.108**
without ZnO/PAAH	46 (75*)	73 (100*)	95	100
With PAAH	< 1	< 1	< 1	3
With ZnO/PAAH	< 1	12	27	48

* after 24 hrs of reaction

The results show first that the kinetics is rather slow, however for practical reasons, in order to carry out all the operations in the same day, coating process should last only 4 hrs. It is obvious that the presence of PAAH inhibits the polycondensation reaction, however too much NH_4OH might cause degradation of the self-assembly system. Our previous studies have shown that the use of an equimolar mixture of PAAH and PAANa or the addition of NaOH during synthesis leads to ZnO/PAA clear suspensions and not to self-assembled structures. [31]

The coating process used here is not expected to affect the inorganic phase. Figure 1 presents the XRD diffractograms of uncoated ZnO/PAA and TEOS-3 nanohybrids. The diffraction peaks of the as-prepared material correspond well to ZnO wurtzite with two impurity peaks at $2\theta = 33.4°$ and 59.4°, related to the polymer (PAAH) as shown in uncoated ZnO/PAA starting materials. The diffractograms show that the presence of the unassigned phase is sensitive to the amount of NH_4OH (Figure 1). The greater the amount of NH_4OH and the weaker the presence of the PAAH crystalline phase. This can be explained by the acid-base reaction of PAAH + NH_4OH which transforms progressively the PAAH into its $PAANH_4$ salt. After calcination at 400 °C, both impurity peaks disappear, confirming that these are most likely related to the organic polymer phase and independent of the introduction of TEOS. No crystalline phase related to silica is observed, suggesting that it probably exists in the amorphous state. Indeed, at the highest ammonia concentration (TEOS-3-4), a broad peak is observed between 25° and 30° in Figure 1 consistent with the presence of amorphous silica.

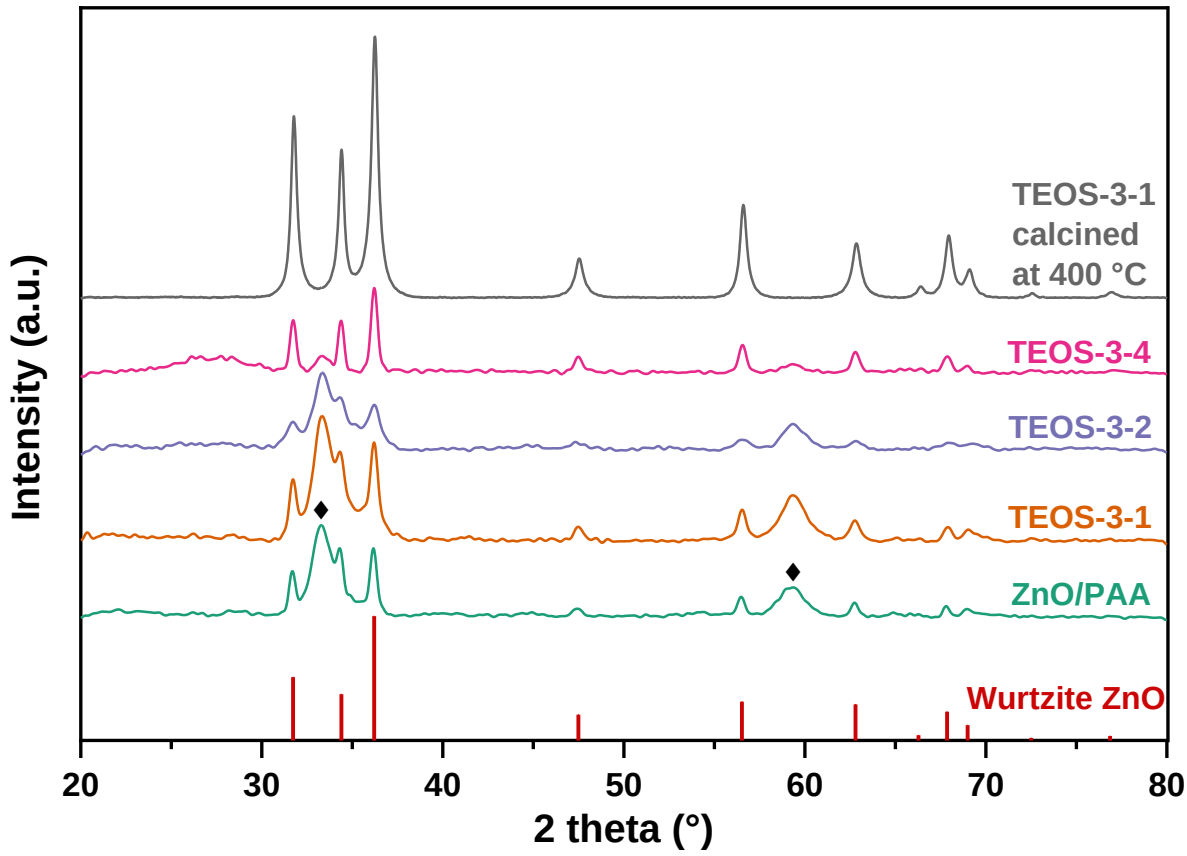

Figure 1: XRD diffractograms of (from bottom to top) uncoated ZnO/PAA, TEOS-3-1, TEOS-3-2, TEOS-3-4 and TEOS-3-1 calcined at 400 °C. The symbols ♦ mark the peaks related to PAA.

The presence of silica is evidenced by FTIR, as illustrated in Figure 2. For both TEOS-3-2 and uncoated ZnO/PAAH samples, the broad feature between 3000 cm^{-1} and 3500 cm^{-1} is associated with water or OH groups. Characteristic PAA bands are observed between 1219 cm^{-1} and 1800 cm^{-1}, including two strong bands at 1551 cm^{-1} and 1408 cm^{-1}, ascribed to the asymmetric and symmetric modes of carboxylate anion (COO^-), respectively. Between 816 cm^{-1} and 1219 cm^{-1}, a broad band is observed for the TEOS-3-2 sample, while it is absent for the uncoated ZnO/PAA. The bands at 1018 cm^{-1} and 945 cm^{-1} are assigned to the asymmetric stretching modes of Si-O-Si vibrations and to the stretching modes of surface silanol groups (≡Si-OH) or even to the vibrational mode of Si-O-Zn, respectively [19,32]. The band at 447 cm^{-1} in ZnO/PAA is attributed to the Zn-O stretching mode, which is a further evidence of the presence of ZnO. Interestingly, it is replaced with a band at 544 cm^{-1} in TEOS-3-2. The position of the Zn-O bond band depends on the size, morphology and axial ratio (c/a) of the ZnO nanocrystals [33]. Oxygen-related defect complexes are also associated with bands close to this range [34]. In agreement with XRD, the band at 544 cm^{-1} is assigned to highly defective ZnO.

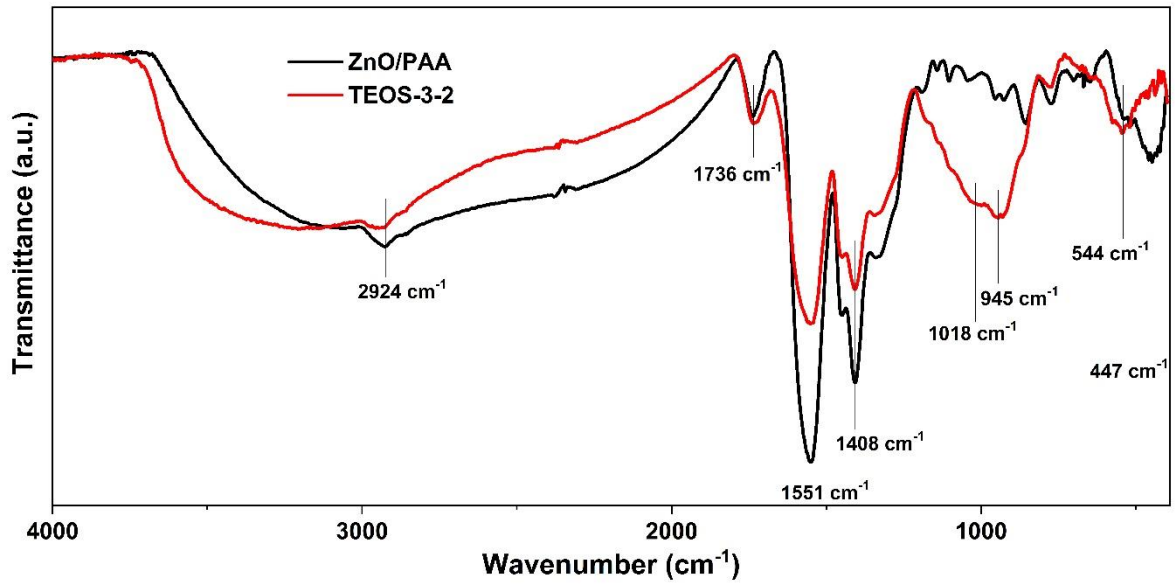

Figure 2: FTIR spectra of the ZnO/PAA and TEOS-3-2 samples.

Figure 3 shows TEM observations of TEOS-3 samples synthesized with different amounts of NH_4OH. For TEOS-3-1 (Figure 3 (a) and (b)), the presence of an amorphous Si-based shell is confirmed around ZnO nanocrystals (Figure 3 (a)). Similarly, it must also be present around PAA mesospheres containing ZnO nanocrystals (Figure 3 (b)), which make the majority of the sample, even though it is hard to obtain an image of a few-nanometer thick silica shell around a 100 nm-thick hybrid structure. The same applies to TEOS-3-2 samples (Figure 3 (c) and (d)). In Figure 3 (d), the ZnO-containing PAA mesospheres are distinguished along with unembedded ZnO nanocrystals around them. For the highest ammonia concentration (four times the nominal amount), the Si-based shell is thicker, which results in a weaker contrast of the ZnO nanocrystals (Figure 3 (e)). More unembedded ZnO nanocrystals can also be observed, suggesting that ammonia at high concentrations disrupts the PAA mesospheres. The effect of ammonia thus appears to be twofold: as its content in solution increases, the successful deposition of silica increases while the mesosphere structures are gradually degraded.

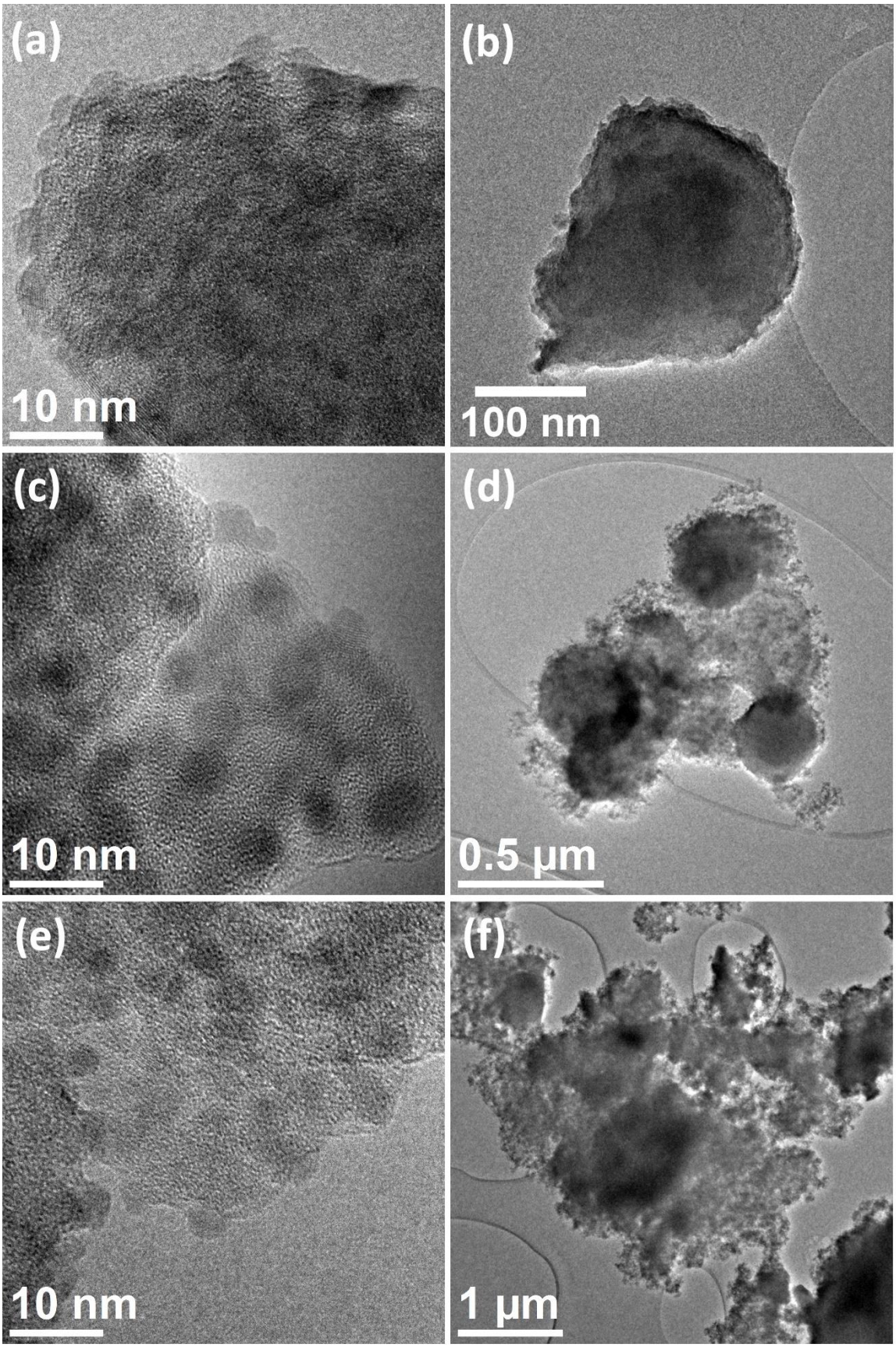

Figure 3: TEM images of TEOS-3 samples with different amount of NH_4OH, (a) (b) TEOS-3-1, (c) (d) TEOS-3-2 and (e) (f) TEOS-3-4.

This statement is confirmed by RBS analysis, the results of which are plotted in Figure 4. A quasi-linear relation exists between the amount of NH_4OH used and the Si:Zn atomic ratio, however these values are very low confirming the low Si content in these materials.

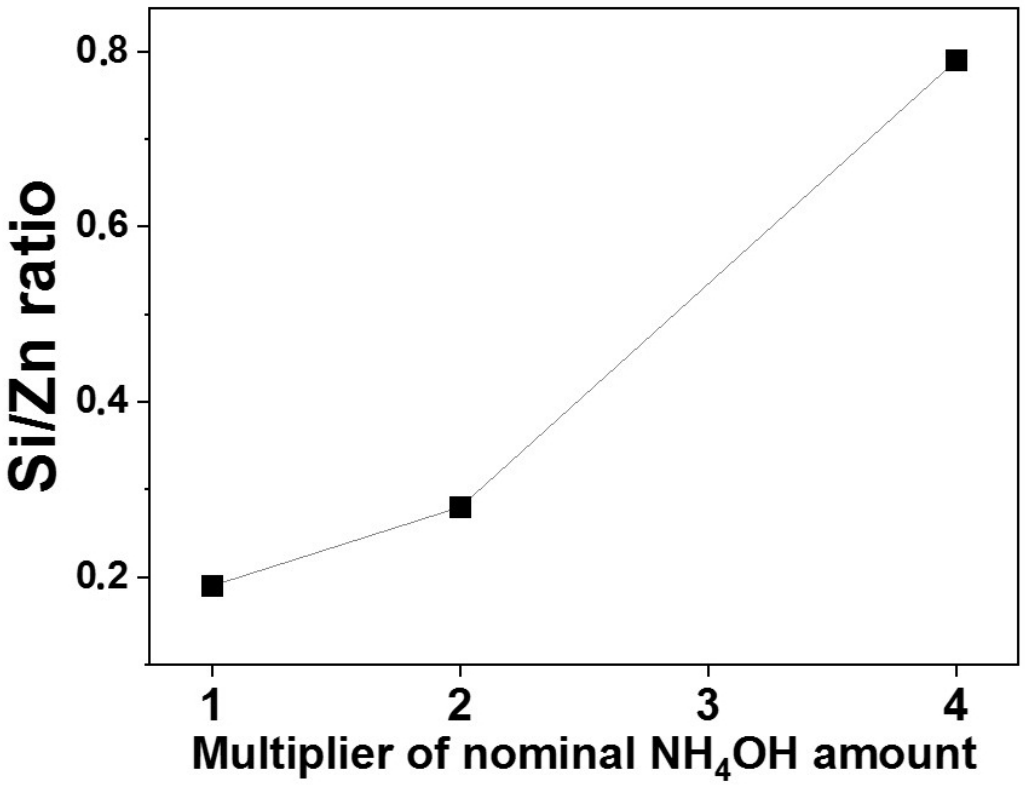

Figure 4: Atomic ratio of Si to Zn in TEOS-3-y samples measured with RBS.

Figure 5 shows representative TEM images of silica-coated ZnO TEOS-3-2 nanostructures. Figure 5 (a) exhibits ZnO/PAA mesospheres decorated with SiO_2 nanoparticles. We intentionally focused our observations on a few ZnO nanocrystals that were not fully embedded in PAA mesospheres. This enabled us to obtain an unambiguous image of the presence of Si-based matrix, since the sample in these regions is much thinner than PAA mesospheres containing ZnO nanocrystals. In the latter case, it would be more difficult to distinguish the Si-based phase from that of the PAA since the PAA mesospheres are rather thick (~ 100 nm) for a high-resolution TEM analysis. It can be clearly seen in Figure 5(b) and (c) that wurtzite ZnO nanocrystals of ~ 5 nm in size are uniformly dispersed in an amorphous matrix. The main statement is therefore that Zn and Si domains are clearly separated. The results obtained by HAADF in a similar region are presented in the inset of Figure 5 (b). The brightest areas of the HAADF image are the signals from the heavier phase (Zn-rich) and the dim areas from lighter ones (Si-rich).

This observation confirms that the light and heavy elements are segregated and in accordance with a coating scenario.

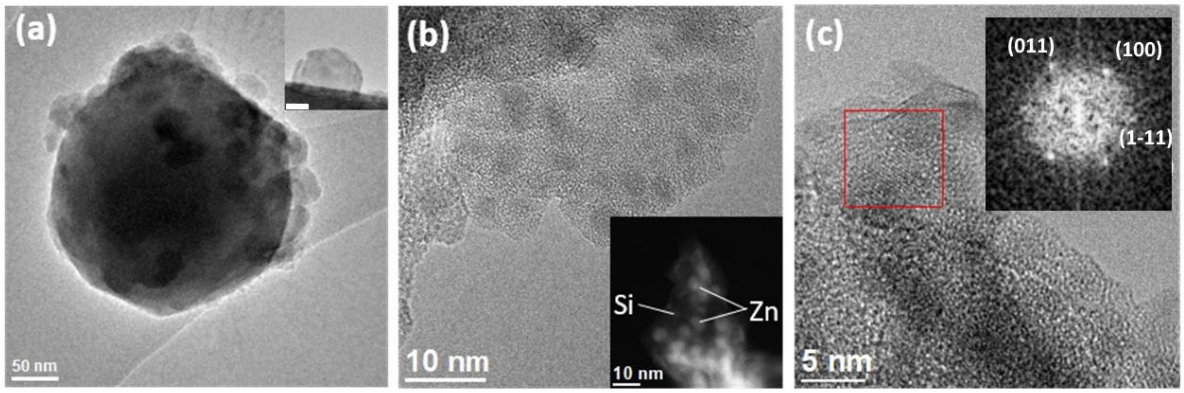

Figure 5: TEM images of TEOS-3-2 (a) silica-decorated ZnO/PAA mesosphere and SiO_2 nanoparticles images (inset, the scale-bar represents 10 nm), (b) TEM showing ZnO nanocrystals in amorphous matrix and HAADF image (inset) evidencing the presence of Si (dim area) and Zn (bright area), and (c) HRTEM image with the inset showing fast Fourier transformed (FFT) image of the red square area of a single ZnO nanocrystal.

Finally, the presence of Si is unambiguously confirmed by EDS (Figure 6). The amorphous coating tentatively assigned to silica contains Si and not Zn. It is difficult to get an absolute composition of the corresponding phases, i.e., to confirm that Si is present in a stoichiometric silica phase. Indeed, oxygen is mapped throughout the sample. Its presence is related to ZnO, the SiO_x phase (with x possibly not equal to 2), PAAH and eventual contamination. However, C map shows significant variations, with higher concentration regions superimposed to Zn rich regions. Combining the elemental maps, the model we can construct is that of ZnO nanocrystals embedded in PAAH mesospheres, the latter being inhomogeneously coated with silica.

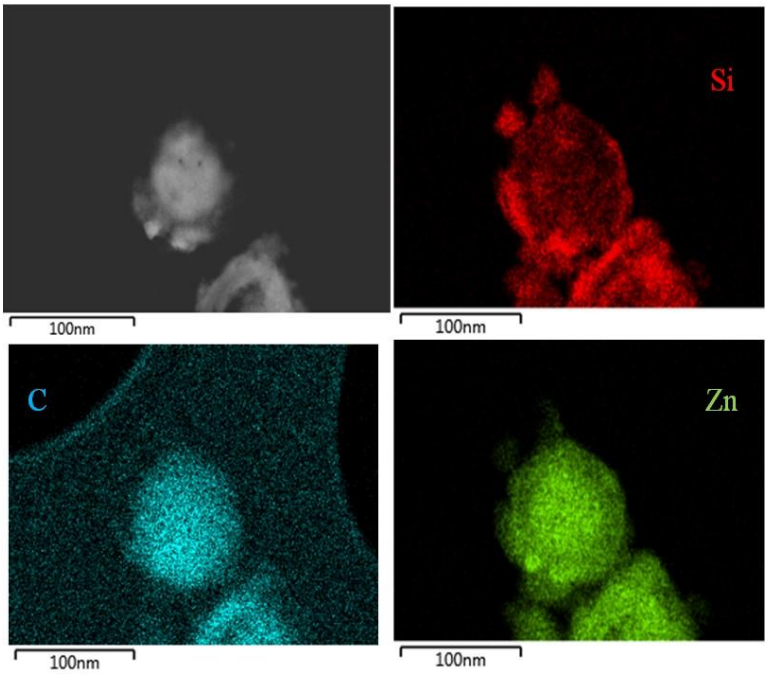

Figure 6: Elemental local analysis of a cluster of ZnO nanocrystals coated with silica in TEOS-3-2 sample. Top left: HAADF image. The other three panels display the elemental maps for Si, C and Zn, respectively.

Keeping the 3D nanostructures self-assembled while elaborating a SiO_2 coating in basic medium proved to be very delicate and only a decoration of these objects could be carried out. At high base concentration, the loss of -COOH functions leads to the destruction of self-assembled nano-objects and the dispersion of ZnO nanocrystals that are gradually incorporated into a SiO_2 matrix (Figure 7).

A key point concerns the role of exposed ZnO, both initially and following the action of ammonia. This exposed ZnO may well act as a nucleation seed for silica. Our observations do not provide definite proof of this hypothesis but will show that it could be so. Indeed, as we add more ammonium, the PAA spheres degrade (see figure 3), exposing more ZnO nanocrystals. At the same time, more silica is produced. Therefore, the effect of ammonia could be two-fold: a direct catalytic effect and a redispersion of the ZnO crystallites, releasing more ZnO seeds. A series of samples with a tunable amount of ZnO nanocrystals may help to investigate this point and identify the important parameters needed to achieve high luminescence performance.

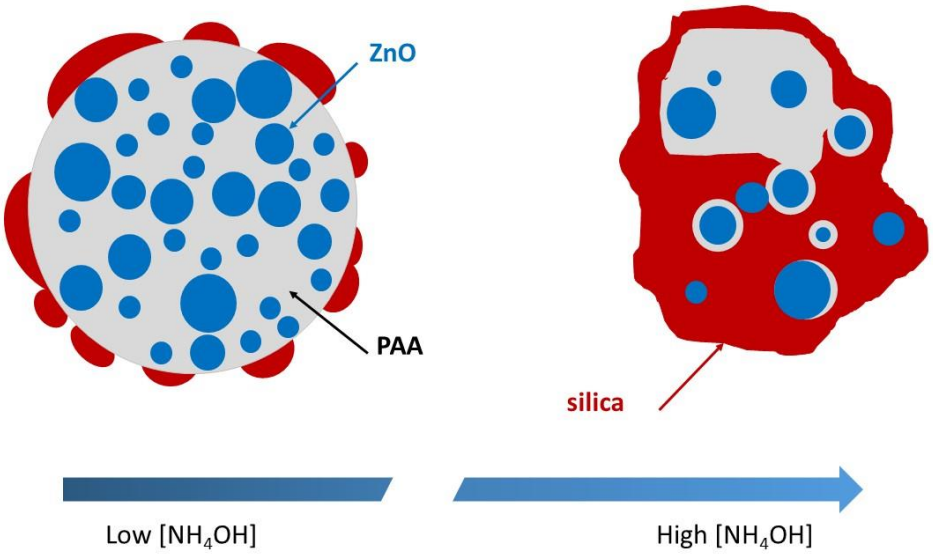

Figure 7: Effect of the [NH_4OH] onto the silica coating of ZnO-PAA mesospheres.

Photoluminescence properties

Effect of silica shell on the photoluminescence spectrum

Regarding the ammonia amount in the coating synthesis, thus the amount of silica in the final samples, the first effect to be probed was on the photoluminescence spectrum. Figure 8 shows the PL spectra of ZnO/PAA, TEOS-3-1 and TEOS-3-2 samples.

In the absence of silica, as already reported in our previous work [26], the PL spectrum peaks at around 2.13 eV. With the addition of silica, the spectrum maximum gradually blue-shifts to blue up to 2.2 eV. This could be due to a reduction of the yellow contribution at ~2 eV, related to the recombination of electrons trapped at zinc interstitials with the deeply trapped holes [35]. However, the main observation is that the silica coating does not significantly modify the spectrum, implying that the nature of the specific crystal defects of ZnO nanocrystals is not affected. The presence of some silica contribution could still be claimed. It is known that under UV excitation, silica can emit visible light in the 1.6 to 2.3 eV range because of defects such as non-bridging oxygen hole center, silylene, silanone or dioxasilyrane [36]. Some of these defects are not stable under ambient conditions while others are. At this stage, the contribution of silica defects cannot be totally ruled out but remains unlikely. Further evidence of the lack of effect of the silica coating on the PL spectra is given in the Supporting Information (Figure SI1).

Regarding the nature of these defects, although there has been a long debate on the defects that could lead to green emission (at or near 2.27 eV), there is now a consensus to consider singly ionized oxygen vacancies as the main cause. Two hypotheses for the corresponding electronic transition are being

debated. For instance, Zeng *et al.* have considered that the green emission results from the de-excitation of electrons from the conduction band and their recombination with holes trapped in deep defects [35]. On the contrary, Camarda *et al.* pointed out that the green emission would rather result from the recombination between a hole of the valence band and an electron deeply trapped at singly-ionized oxygen vacancy [37]. Based on the most recent analyses, we would favor the second hypothesis. Whatever the exact transition, oxygen vacancies are intimately linked to the generation of a green visible emission in our nanohybrids. The fact that the silica coating does not modify the spectrum suggests that the PAA spheres, embedding the emitting ZnO nanocrystals, does not allow easy diffusion of oxygen-related species from the reaction solution of directly from the silica coating.

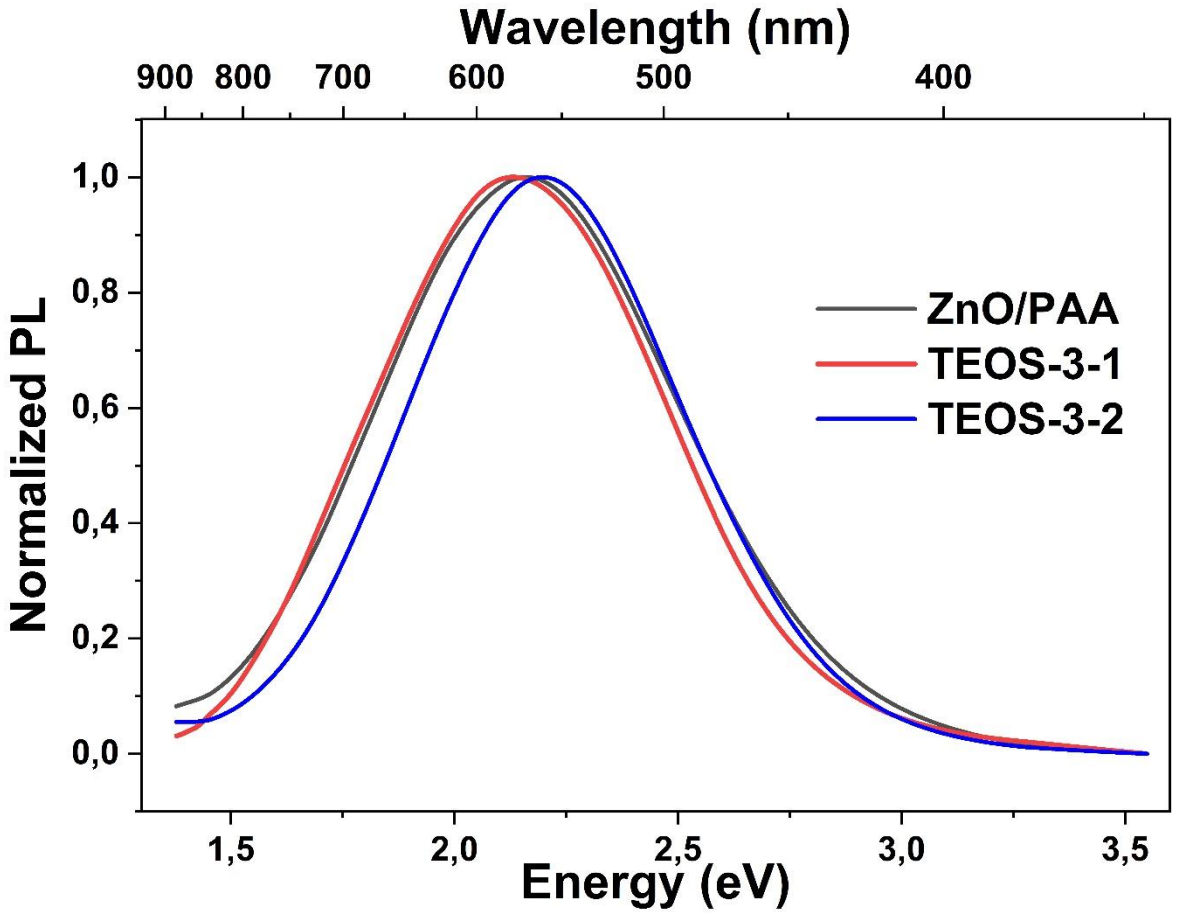

Figure 8: Normalized PL spectra of ZnO/PAA, TEOS-3-1 and TEOS-3-2 samples.

We then checked the effect of the silica coating on the excited states responsible for PL by performing PL excitation (PLE) experiments on samples prepared with different amounts of ammonia. The results, uncorrected for the absorption profile, are presented in Figure 9 for ZnO/PAA, TEOS-3-1 and TEOS-3-2 samples. The PLE spectrum of ZnO nanocrystals embedded in PAA, in the absence of silica,

reproduces the one we measured in our previous work [26] and is consistent with PLE spectra reported for other ZnO nanocrystals [35,37]. The visible emission is essentially generated by absorption across the band gap for wavelengths above 365 nm. A first optimum is obtained at 330 nm, comparable to the maximum at 335 nm observed in [35]. A second optimum is obtained at 255 nm. The latter could be partially related to absorption by the surrounding PAA followed by charge transfer to the embedded ZnO nanocrystals.

No modification in the PLE spectra is observed for once or twice the nominal amount of ammonia, meaning that for such ammonia concentrations no change in the PL path is induced. Hence, neither the nature of the defects responsible for visible luminescence nor the way energy is transferred to these emitting defects in these cases are affected. In particular, we can rule out any energy transfer from silica coating to ZnO nanocrystals. It is likely that the excitation energy is partially absorbed directly by the ZnO nanocrystals and partially absorbed by the PAA spheres. In the first case, the absorption leads to direct visible emission while in the second case, the emission is mediated by energy or charge transfer from the PAA matrix to the ZnO nanocrystals.

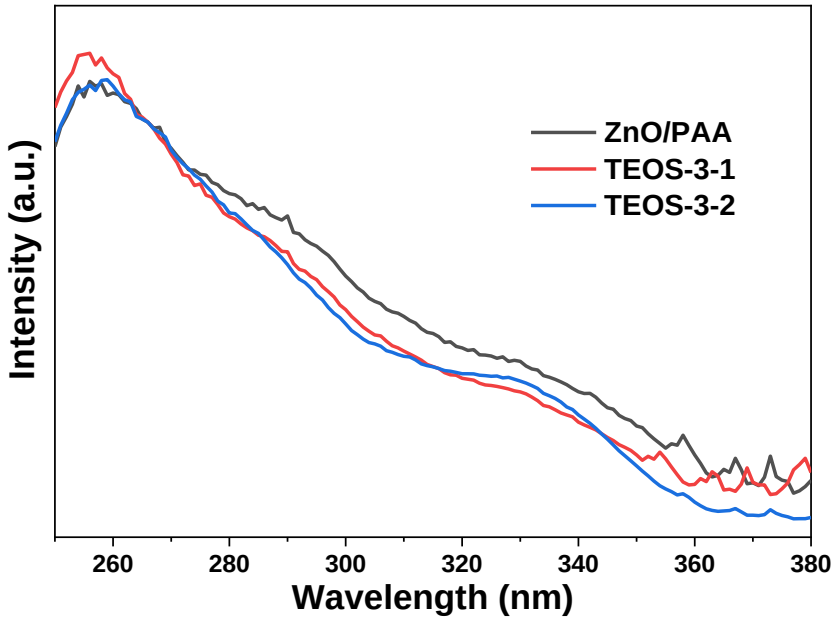

Figure 9: PLE spectra at λ_{em} = 550 nm of ZnO/PAA, TEOS-3-1 and TEOS-3-2 samples with different amounts of NH_4OH. The spectra are normalized to the intensity at λ_{ex} = 266 nm.

Effect of silica shell on the photoluminescence quantum yield

We studied the PL QY variation of silica-coated nanohybrids with respect to their uncoated counterparts, synthesized in the same way at the initial step of synthesis. The only difference is thus due to the silica coating. Figure 10 shows PL QY for all silica-coated samples with an optimum for TEOS-3-2 (see also

figure SI2). The PL QY is considerably improved by almost six-fold with the absolute value of PL QY increasing from 8.9 % to 64.0 %. We checked that the presence of ammonia (at twice the nominal concentration), during the process without TEOS injection, does not modify the PL QY of the initial samples and thus that ammonia is not responsible for any PL QY modification. This enables us to completely rule out the possible contribution of silica defects to the visible emission.

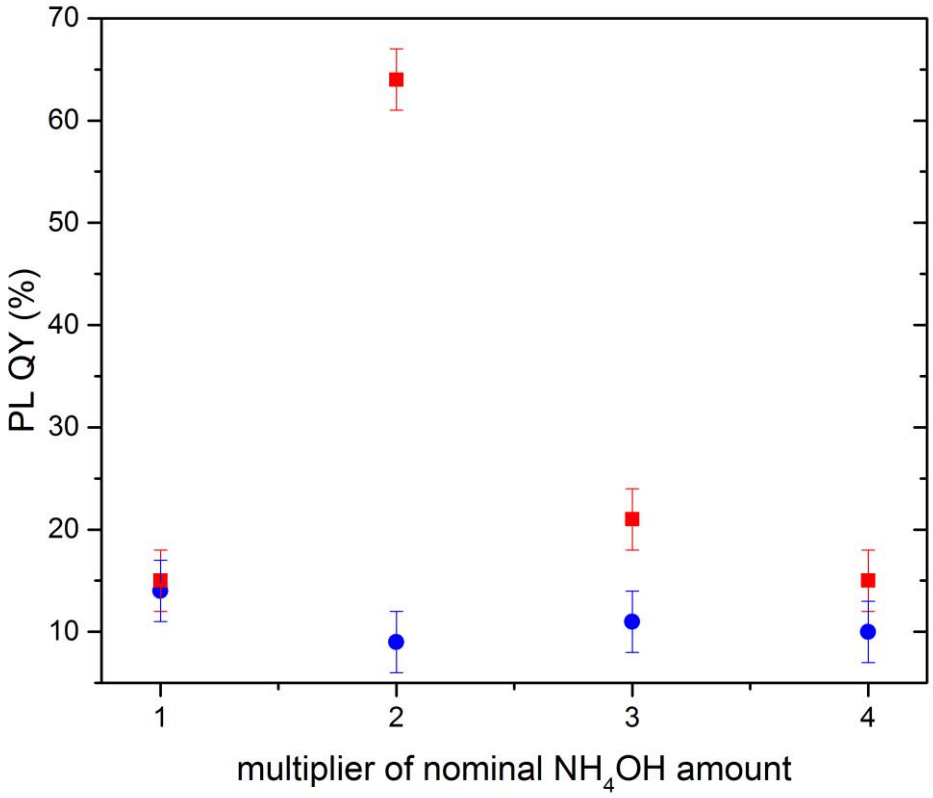

Figure 10: PL QY of TEOS-3 samples with different amount of NH_4OH before (blue circles) and after (red squares) the deposition of the silica coating.

A miscellaneous effect of silica on PL QY improvement could be that the initial samples contain ZnO nanocrystals that are not embedded in the PAA mesospheres, either initially or as a result of the action of ammonia. These non-passivated nanocrystals are mostly ineffective for PL. After coating with silica, they could be passivated and begin to emit visible light more efficiently, along with the ZnO nanocrystals embedded in silica-coated PAA mesospheres. Although we expect this effect to be minor and despite the fact that the silica coating on bare ZnO nanocrystals often quenches the visible luminescence, we cannot entirely rule it out.

In Figure 10, two antagonistic effects of silica coating can be noticed. As the silica amount increases, the coverage of the mesosphere increases while preserving the integrity of the mesospheres that are

beneficial for light trapping and scattering (see previous sections). This improves the protection of the nanohybrids (possibly from moisture or contaminant). At large ammonia concentrations, the detrimental effect is twofold. On the one hand, ammonia degrades the integrity of the mesospheres while on the other hand the silica coating grows thicker. This induces some absorption of the excitation light by the silica coating and less by the ZnO/PAA nanohybrids. Consequently, the PL QY of the overall system decreases. An optimum in silica coating is thus to be achieved.

The exact mechanism responsible for the PL QY improvement remains elusive. However, two complementary hypotheses can be put forward. The first one consists in the feeling?? of pores present in the PAA spheres. The mesospheres would therefore no longer be permeable to the ambient contaminant, or to the contaminant of the synthesis solution which could quench some of the defects (i.e. essentially oxygen vacancies) necessary for visible emission of ZnO. The second hypothesis is based on an electronic argument. The visible emission in ZnO nanocrystals is essentially due to singly ionized oxygen vacancies (Vo). We have previously stated that the nature of the defects responsible for the visible emission is not disturbed by the introduction of TEOS. However, either the overall concentration of V_O, or more likely, the concentration of singly ionized V_O could be increased by the introduction of TEOS and the resulting synthesis of silica. It seems difficult to imagine that TEOS would actually induce the formation of oxygen vacancies with ZnO nanocrystals embedded in PAA mesospheres. However, since the PAA mesospheres are not impermeable to charge migration, a change of the charge state of oxygen vacancies of some of the ZnO nanocrystals can be considered, which would lead to an increase in the singly ionized Vo concentration.

Effect of silica shell on the photoluminescence performances as function of temperature

In the perspective of using such coated nanohybrid mesospheres in WLED applications, their PL performance has been studied as a function of operating temperature. The spectra evolutions are presented in Supporting Information (figure SI3) and summed up in Figure 11.

The first observation is that increasing the temperature to 100 °C, a typical operation temperature in WLEDs, leads to a reduction in luminescence intensity by a factor of about five for the uncoated sample and by a factor of three for the coated samples. Second, when the sample is cooled to room temperature (in cycles), the recovered PL intensity amounts to approximately 75 % of the initial one. This value is independent of the coating as can be observed from the temperature evolution of the normalized PL intensity in Figure 11. The main difference between the samples is the absolute value of the intensity at room temperature, the PL QY of the TEOS-3-2 sample being substantially higher than that of the uncoated one as shown in figure 10. Therefore, the thermal quenching of the PL, which would otherwise be detrimental to the application of uncoated mesosphere samples in devices operating at high

temperature, has a reduced impact for the application of coated samples, leaving sufficient light produced at 100 °C.

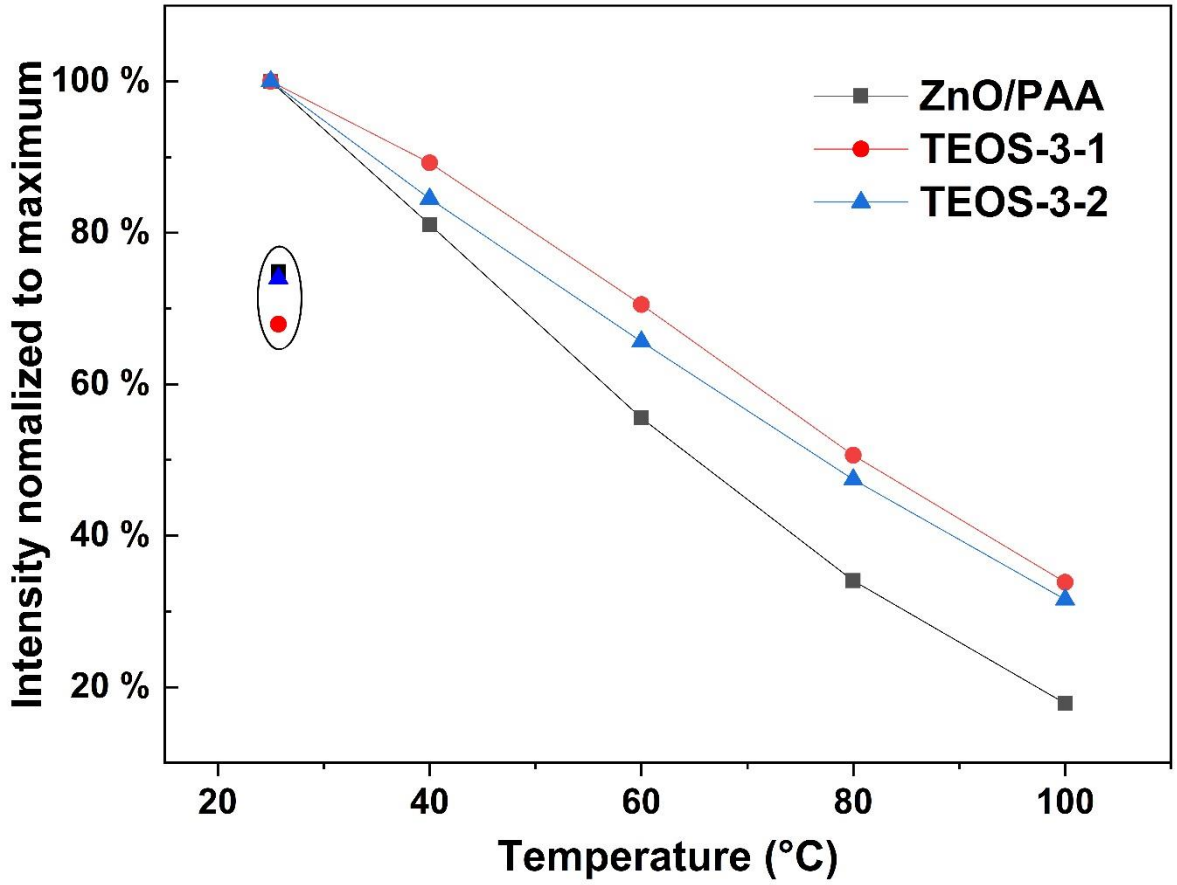

Figure 11: Evolution of the normalized PL intensity ZnO/PAA, TEOS-3-1 and TEOS-3-2 at different temperatures from 25 °C to 100 °C. The circled labels refer to the values reached after cooling back to room temperature.

Conclusions

In conclusion, we have demonstrated that the silica coating of our ZnO/PAA nanohybrids is strongly affected by the amount of NH_4OH used. This reagent has two antagonistic effects since it improves the polycondensation kinetics of silica but at high concentration, NH_4OH can disrupt the stability of the initial ZnO/PAA mesospheres, by degrading their integrity. At the same time, the resulting silica layer thickens and partly absorbs the UV excitation light, preventing it from exciting the ZnO nanocrystals embedded in the PAA mesospheres. As a result, part of the excitation light is lost in the coating, resulting in a decrease in PL QY. However, whatever the ammonia content in the synthesis solution, the PL QY

of the resulting silica coated samples is always improved as compared to the uncoated counterparts. Therefore, a silica shell around the nanohybrid mesospheres is beneficial, leading, in the optimal case, to significant, robust and competitive PL QY over 60%. The mesospheres have a beneficial effect on the scattering and trapping of light in the sample thus improving the light absorption. An intermediate situation that is more akin to a surface decoration of these objects seems to be the best compromise between maintaining self-assembly and improving optical performances. However, this coating does not make it possible to improve the thermal performance of these nano-objects, which is an area for further improvement.

Acknowledgements

Y. Z. is grateful to the CSC for Ph-D scholarship. The authors acknowledge the Consortium Lyon Saint-Etienne de Microscopie (CLYM) for TEM measurements, the IP2I laboratory (Université de Lyon) for RBS measurements and Prof. C. Dujardin's team (ILM, Université de Lyon) for technical assistance in the temperature PL measurements.

[1] F. Jelezko, J. Wrachtrup, "Single defect centres in diamond : A review", *Physica Status Solidi A* **203**,3207-3225 (2006)
[2] R. Schirhagl, K. Chang, M. Loretz, C. L. Degen, "Nitrogen-Vacancy Centers in Diamond : Nanoscale Sensors for Physics and Biology", *Annual Review of Physical Chemistry* **65**, 83-108 (2014)
[3] I. Aharonovich, S. Casteletto, D. A. Simpson, C-H. Su, A. D. Greentree, S. Prawer, "Diamond-based single-photon emitters", *Reports on Progress in Physics* **74**, 076501 (2011)
[4] A. Lohrmann, B. C. Johnson, J. C. McCallum, S. Casteletto, "review on single photon sources in silicon carbide", *Reports on Progress in Physics* **80**, 034502 (2017)
[5] Tang X. S., Choo E. S. G., Li L., Ding J., Xue J. M., "Synthesis of ZnO Nanoparticles with Tunable Emission Colors and Their Cell Labeling Applications", *Chem. Mater.* **22**, 3383-3388 (2010).
[6] P. Felbier P. J. Yang, J. Theis, R. W. Liptak, A. Wagner, A. Lorke, G. Bacher, U. Kortshagen, "Highly Luminescent ZnO Quantum Dots Made in a Nonthermal Plasma". *Adv. Func. Mat*., **24**, 1988-1993 (2014).
[7] H. M. Xiong R. Z. Ma S. F. Wang Y. Y. Xia, "Photoluminescent ZnO nanoparticles synthesized at the interface between air and triethylene glycol" *J. Mater. Chem.* **21**, 3178-3182 (2011).
[8] Y.-S. Fu X. W. Du , S. A. Kulinich, J. S. Qiu, W. J. Qin , R. Li, J. Sun, J. Liu, „Stable aqueous dispersion of ZnO quantum dots with strong blue emission via simple solution route", *J. Am. Chem. Soc.* **129**, 16029– 16033 (2007).
[9] S. Choi, A. M. Berhane, A. Gentle, C. Ton-That, M. R. Phillips and I. Aharonovich, "Electroluminescence from isolated defects in zinc oxide – towards electrically triggered single photon sources at room temperature", *ACS Appl. Mat. & Int.* **7**, 5619-5623 (2015).
[10] A. J. Morfa, B. C. Gibson, M. Karg, T. J. Karle, A. D. Greentree, P. Mulvaney and S. Tomljenovic-Hanic, "Single-photon emission and quantum characterization of zinc oxide defects", *Nano Lett.* **12**, 949-954 (2012).
[11] M. D. McCluskey and S. J. Jokela, Defects in ZnO, *J. Appl. Phys.* **106**, 071101 (2009).
[12] M. L. Kahn, T. Cardinal, B. Bousquet, M. Monge, V. Jubera, B. Chaudret, "Optical properties of zinc oxide nanoparticles and nanorods synthesized using an organometallic method", *ChemPhysChem* **7**, 2392-2397 (2006)
[13] Z. G. Wang, X. T. Zu, S. Zhu, L. M. Wang, "Green luminescence originates from surface defects in ZnO nanoparticles", *Physica E* **35**, 199-202 (2006).
[14] H. Zeng, G. Duan, Y. Li, S. Yang, X. Xu W. Cai, "Blue luminescence of ZnO nanoparticles based on non-equilibrium processes: defect origins and emission controls", *Adv. Funct. Mater.* **20**, 561-572 (2010).
[15] M. A. Reshchikov, H. Morkoç, B. Nemeth, J. Nause, J. Xie, B. Hertog, A. Osinsky, "Luminescence properties of defects in ZnO", *Physica B* **401-402**, 358-361 (2007).

[16] N. S. Norbert, D. R. Gamelin, "Influence of Surface Modification on the Luminescence of Colloidal ZnO Nanocrystals", *J. Phys. Chem. B*, **109**, 20810 (2005).

[17] D. Tainoff, B. Masenelli, O. Boisron, G. Guiraud, P. Melinon, "Crystallinity, Stoichiometry and luminescence of high quality ZnO nanoclusters"*, J. Phys. Chem. C* **112**, 12623-12627 (2008).

[18] J. Zhai, X. Tao, Y. Pu, , X. F. Zeng, and J. F. Chen, "Core/shell structured ZnO/SiO_2 nanoparticles: Preparation, characterization and photocatalytic property". *Applied Surface Science* **257** (2), 393-397 (2010).

[19] K. S. Babu, A. R. Reddy, and K. V. Reddy, "Controlling the size and optical properties of ZnO nanoparticles by capping with SiO_2." *Materials Research Bulletin* **49**, 537-543 (2014).

[20] I. M. El-Nahhal, J. K. Salem, S. Kuhn T. Hammad, R. Hempelmann, and S. Al Bhaisi, "Synthesis & characterization of silica coated and functionalized silica coated zinc oxide nanomaterials", *Powder technology* **287**, 439-446 (2016).

[21] M. Ramasamy, Y. J. Kim, H. Gao, D. K. Yi and J. H. An, "Synthesis of silica coated zinc oxide–poly (ethylene-co-acrylic acid) matrix and its UV shielding evaluation", *Materials Research Bulletin* **51**, 85-91. (2014).

[22] E. Tang and S. Dong, "Preparation of styrene polymer/ZnO nanocomposite latex via miniemulsion polymerization and its antibacterial property", *Colloid and Polymer Science* **287** (9), 1025-1032 (2009).

[23] N. Hagura, T. Takeuchi, S. Takayama, F. Iskandar and K. Okuyama, "Enhanced photoluminescence of ZnO–SiO_2 nanocomposite particles and the analyses of structure and composition." *Journal of Luminescence* **131** (1), 138-146 (2011).

[24] Y. Y. Peng, T. E. Hsieh and C. H. Hsu, "White-light emitting ZnO–SiO_2 nanocomposite thin films prepared by the target-attached sputtering method". *Nanotechnology* **17** (1), 174 (2005).

[25] R. G. Singh, F. Singh, D. Kanjilal, V. Agarwal and R. M. Mehra, "White light emission from chemically synthesized ZnO–porous silicon nanocomposite", *Journal of Physics D: Applied Physics* **42** (6), 062002 (2009).

[26] Y. Zhu, A. Apostoluk, P. Gautier, A. Valette, T. Cornier, J. Bluet, K. Masenelli-Varlot, S. Danièle, B. Masenelli, "Intense visible emission from ZnO/PAAX (X = H or Na) nanocomposite synthesized via a simple and scalable sol-gel method". *Scientific reports* **6**, 23557 (2016).

[27] M. Fuji C. Takai, H. Imabeppu and X. Xu, "Synthesis and shell structure design of hollow silica nanoparticles using polyelectrolyte as template", *J. Phys.: Conf. Ser.* **596** 012007 (2015).

[28] Y. Wan and S.-H. Yu, "Polyelectrolyte controlled large-scale synthesis of hollow silica spheres with tunable sizes and wall thicknesses", *J. Phys. Chem. C* **112**, 3641-3647 (2008).

[29] Y. Zhang, A. Apostoluk, C. Theron, T. Cornier, B. Canut, S. Daniele, B. Masenelli, "Doping of ZnO inorganic-organic nanohybrids with metal elements", *Scientific Reports* **9**, 11959 (2019).

[30] J. C. de Mello, H. F. Wittmann, and R. H. Friend. "An improved experimental determination of external photoluminescence quantum efficiency". *Advanced materials* **9**, 230-232 (1997).

[31] S. Daniele, A. Valette, T. Cornier, Patent PCT WO 2016/038317 A1

[32] F. El-Kabbany, S. Taha, M. Hafez and I. S. Yahia, "Thermal and spectroscopic properties of the nano-system ($ZnO_{(1-x)}$ $SiO_{2(x)}$)", *Journal of Molecular Structure* **1111,** 33-45 (2016).

[33] B. H. Soni, M. P. Deshpande, S. V. Bhatt, N. Garg, and S. H. Chaki, "Studies on ZnO nanorods synthesized by hydrothermal method and their characterization", Journal of Nano- and Electronic Physics 5 (4), 04077-6 (2013).

[34] G. Xiong, U. Pal, J. G. Serrano, K. B. Ucer, R. T. Williams, "Photoluminescence and FTIR study of ZnO nanoparticles: the impurity and defect perspective", *Phys. Stat. Sol. C* **3**, 3577-3581 (2006).

[35] H. Zeng, G. Duan, Y. Li, S. Yang, X. Xu, W. Cai, "blue luminescence of ZnO nanoparticles based on non-equilibrium processes: defect origins and emission controls",Adv. Funct. Mater. **20**, 561-572 (2020).

[36] L. Vaccaro, A. Morana, V. Radzig, M. Cannas, "Bright visible luminescence in silica nanoparticles", J. Phys. Chem. C **115**, 19476-19481 (2011).

[37] P. Camarda, F. Messina, L. Vaccaro, S. Agenllo, G. Buscarino, R. Schneider, D. Gerthsen, R. Lorenzi, F. M. Gelardi, M. Cannas, "Luminescence mechanisms of defective znO nanoparticles", Phys.Chem.Chem.Phys. **18**, 13237 (2016).